

# Replica Symmetry Breaking in

## FRET-assisted Random Laser Based on Electrospun Polymer Fiber

Jiangying Xia,<sup>1,†</sup> Jijun He,<sup>4,†</sup> Kang Xie<sup>1,†</sup> Xiaojuan Zhang,<sup>3</sup> Lei Hu,<sup>1</sup> Yaxin Li,<sup>1</sup> Xianxian Chen,<sup>1</sup> Jiajun Ma,<sup>2</sup> Jianxiang Wen,<sup>5</sup> Jingjing Chen,<sup>1</sup> Qiaosheng Pan,<sup>1</sup> Junxi Zhang,<sup>1</sup> Ilya D. Vatnik<sup>6</sup>, Dmitry Churkin<sup>6</sup> and Zhijia Hu,<sup>1,2,3,5,\*</sup>

<sup>1</sup>*School of Instrument Science and Opto-electronics Engineering, Hefei University of Technology, Hefei, Anhui 230009, P. R. China*

<sup>2</sup>*State Key Laboratory of Environmental Friendly Energy Materials, Southwest University of Science and Technology, Mianyang, Sichuan 621000, P. R. China*

<sup>3</sup>*Aston Institute of Photonic Technologies, Aston University, Birmingham B4 7ET, United Kingdom*

<sup>4</sup>*Department of Electrical Engineering, the Hong Kong Polytechnic University, Kowloon 99077, Hong Kong, P. R. China*

<sup>5</sup>*Key Laboratory of Specialty Fiber Optics and Optical Access Networks, Shanghai University, Shanghai, 200072, P. R. China*

<sup>6</sup>*Institute of Automation and Electrometry SB RAS, Novosibirsk 630055, Russia*

<sup>†</sup>Jiangying Xia, Jijun He, and Kang Xie contributed equally to this work

\*E-mail addresses: [zhijiahu@hfut.edu.cn](mailto:zhijiahu@hfut.edu.cn) (Z.-J. Hu)

Spin-glass theory has been widely introduced to describe the phase transition and statistical behaviors in the complex physical systems, such as, condensed matter, ecological community and even financial market. By the analogy between disorder photonics and other complex systems, the glassy behavior, especially the replica symmetry breaking (RSB) phenomenon, has been observed in an unconventional laser system, i.e. random lasers. However, previous studies only analyzed the statistical properties of the random laser systems with single gain material. Here we report the first experimental evidence of the glassy behavior in a random laser with more complex energy level structure. This novel random laser is demonstrated based on the electrospun polymer fibers with the assistant of Förster resonance energy resonance energy transfer (FRET). The electrospun technology employed in our experiment promises high-volume production of random laser devices with multiple types of the laser dyes, enabling the comprehensive investigation of lasing properties in multi-energy level random laser system. Clear paramagnetic phase and spin-glass phase have been observed in the FRET-assisted random laser under different pump energy. The RSB phase transition is verified to be occurred at the laser threshold, which is robust among the random lasers with different donor-acceptor ratio. The findings of RSB in FRET-assisted random laser enriches the physical theories in the research field of the random laser and provides a new statistical analysis method towards the laser system with complex energy level, e.g. quantum cascade laser.

## 1. Introduction

Since the concept of random lasers (RLs) was proposed in 1995,<sup>[1,2]</sup> they have drawn widespread attention from the laser research communities due to their unique properties (e.g. low spatial coherent and compact device configuration) and various potential applications.<sup>[3-6]</sup> Different from the traditional laser system, RLs do not have well-defined laser cavities and their lasing feedbacks are simply provided by the multiple light scattering. This cavity-less feature enables the easy realization of RLs based on the various disorder systems, such as liquid crystal,<sup>[7,8]</sup> thin polymer film,<sup>[9,10]</sup> quartz tube<sup>[11,12]</sup> and polymer fiber.<sup>[13,14]</sup> Moreover, due to the modifiability of RLs, many studies have been devoted to functionalize the RLs system with special characteristics such as multi-color emission and tunable lasing wavelengths.<sup>[15,16]</sup> Wavelength-tunable RLs recently have attracted intense interest, because they show great promise for various fields, from spectroscopy to photochemistry and medicine.<sup>[17]</sup> Particularly, in the field of medicine and biology, long-wavelength ( $\geq 650$  nm) lasers play an irreplaceable role due to their high penetrability and low sample photo-damage.<sup>[18]</sup> Generally, in dye laser systems, the standard pump source is the frequency-doubled Nd:YAG light with a emission wavelength of 532 nm. However, the commercial long-wavelength ( $\geq 650$  nm) laser dyes show relatively low absorption cross sections at such pumping wavelength, which limits the lasing efficiency and hinders the development of long-wavelength lasers. One effective way to overcome this limitation is to construct a laser system with the assistant of Förster resonance

energy transfer (FRET) between several different types of laser dyes (i.e. donor and acceptor).<sup>[19]</sup> The FRET process occurs when the emission of a donor has a large spectral overlap with the absorption of a nearby acceptor. The donor at excited state will non-radiatively transfer its energy to the acceptor at ground state and promote the excitation of the acceptor.<sup>[20]</sup> As a result, a wavelength-tunable laser system can be achieved via choosing suitable laser dyes and controlling their doping ratio. A number of FRET-assisted RLs have been established in various systems such as biopolymeric matrix dye-doped latex nanoparticles and plasmonic nanostructures.<sup>[21-23]</sup> However, these FRET systems are too complicated to achieve mass production with low cost. In 2010, Vohra and co-workers shows that a FRET system can be easily and effectively fabricated based on the polymeric nanofibers via electrospun technology.<sup>[24]</sup> This electrospun technology is particularly promising in the field of photonics, since it offers a flexible approach to select the optical refractive index, gain and absorption of the fibers. These electrospun polymer fibers and fiber networks also hold great promising in the applications of sensing<sup>[25,26]</sup> and tissue-growth.<sup>[27,28]</sup> Although electrospun polymer fiber have been demonstrated to be an ideal FRET systems, to the best of our knowledge, only energy transferred fluorescence emission has been observed in previously reports.<sup>[24,29-30]</sup>

In the RL systems, one important feature is the intrinsic spectral intensity fluctuation. This spectral intensity fluctuation behavior is rich in the physical mechanism reflecting the

interaction between the nonlinearity and randomness in the RL systems, which have been lately exploited in several studies. In these studies, the replica symmetry breaking (RSB) phenomenon, an important concept in the spin-glass theory, has been observed among different RL systems. Spin-glass theory is one of the primary physics mechanism in many research fields, such as biological systems, ultracold atoms, and random photonics.<sup>[31-33]</sup> Based on the prediction of the spin-glass theory from the equilibrium perspective, the identical systems may reach different states under identical conditions. The transition to a glassy state is known as RSB, which is indicated by the variation of the statistical distribution of the Parisi overlap (i.e. order parameter). The first theoretical models that introduced the term of spin-glass into the photonic context was proposed by Angelani and co-workers. They demonstrated that the light propagation in nonlinear disordered media shows complex glassy behavior and they theoretically predicted that RSB can be tested in RL systems.<sup>[34,35]</sup> In 2015, the first experimental evidence of the RSB in RL was reported by Ghofraniha *et al.*,<sup>[37]</sup> in which the spectral intensity fluctuation overlap (IFO) is defined to as an analog to the Parisi overlap parameter. It was found that the statistical property of IFO exhibited the spin-glass phase behavior under high pump energy, whereas it became paramagnetic phase at low pump energy. The phase transition occurred at the laser threshold. In the same year, a comprehensive disordered mean-field model was presented by Antenucci F. *et al.*, describing the complete phase diagram from close cavity to open cavity in terms of disorder

strength and nonlinearity within the replica analysis. They also theoretically predicted the RSB phase transition can be found in a RL system with quenched disorder.<sup>[38]</sup> Thereafter, many studies reported that the RSB phenomenon can be observed in different RL system with different configuration such as Er-doped fiber laser with random grating,<sup>[39]</sup> Rhodamine B laser dye soliton with ZnO nanoparticles,<sup>[40]</sup> and Rhodamine 6G laser dye soliton with specially designed TiO<sub>2</sub> nanoparticles.<sup>[41]</sup> Thus, using spin-glass theory to analysis the statistical behavior of the RL system provides a new approach to understand the physical mechanism inside the RL. For example, it was found that the spin-glass phase also corresponds to the previously reported Levy distribution regime in RL systems. However, all the previous studies of RSB phenomenon in RLs were demonstrated in a single gain system. For the FRET-assisted RLs, two or more gain materials (donor and acceptor) co-exist in the system and form a multiple energy level configuration. The energy transfer between the doped dyes might modify the nonlinearity of the whole systems and further influence the statistical behavior of the RL system. However, the corresponding statistical study has not been conducted yet. The feasibility of using spin-glass theory to statistical investigate the multi-energy level photonic system like FRET-assisted RL remains a question.

In this work, an advanced electrospun technology is employed to prepare micro-scale polymer fiber, which serves as the framework of FRET system. The gain materials in this FRET system is consist of two laser dyes: pyrromethene 597 (PM597) as the donor and nile blue

(NB) as the acceptor. Due to the multiple light scattering provided by the inhomogeneous internal structure of the electrospun polymer fiber, the random lasing behavior has been observed in our FRET system. The lasing wavelengths are located in two spectral bands, corresponding to the emission of the PM597 and NB dyes, respectively. When the PM597/NB ratio is 0.67/1, only the random lasing with wavelength centered at 685 nm appear in the lasing spectra, which indicates the occurrence of energy transfer from PM597 to NB. Furthermore, it is found that the mass ratio of PM597/NB has an obvious influence on the relative lasing intensity between two lasing wavelength bands, reflecting the variation of the energy transfer degree. In view of this, FRET-assisted RL is successfully demonstrated based on electrospun polymer fiber. To further analyze the statistical properties of RL, we calculated the statistical distribution function  $P(q)$  of the IFO parameter  $q$ . A clear transition, that is the RSB, between a continuous wave paramagnetic regime and a spin-glass phase has been observed in the FRET-assisted RL. The statistical results prove that the spin-glass theory can be used to describe the multi-energy level photonic system. The relationship between the FRET-assisted RL and the single gain RL regarding to the statistical properties of the lasing intensity fluctuation has been discussed, which helps people to better understand the inner link between the spin-glass system and RL in the aspect of statistical physics.

## 2. Materials and methods

The advanced technology-electrospun is introduced to fabricate micro-scale polymer fiber. Firstly, four electrospun sample solutions with same amount of host materials and different PM597/NB mass ratio were prepared. The host materials were obtained via dissolving wt. % 33.4 poly(methyl methacrylate) (PMMA) in wt. % 0.3 PM597/NB-doped dichloromethane ( $\text{CH}_2\text{Cl}_2$ ). The mass ratio of PM597/NB for the four samples was adjusted to be 0.67/1, 1/1, 1.5/1, and 3/1, respectively. Secondly, the as-prepared four sample solutions were used to fabricate four micro-scale polymer fibers samples by the electrospun method.<sup>[42]</sup> A metal needle attached with a 5 ml syringe containing the spinning solution worked as the positive electrode and a high voltage about 10 KV was applied on it. The inside diameter of the metal needle is about 0.9 mm. The grounded electrode was connected to a metal collector covered with metal wafer (20×40 cm). The distance between the needle tip and the collector was fixed at 20 cm. The feed rate of solutions was controlled at 0.8 mm/min by means of a single syringe pump. Figure 1 shows the optical images of two dye doped-electrospun polymer fibers with PM597/NB mass ratio of 0.67/1 and 1.5/1 under the pump of 532 nm pulse laser. The diameters of these two samples are about 218  $\mu\text{m}$  and 248  $\mu\text{m}$ , respectively. Moreover, it clearly shows the location of laser pumping and the fluorescent emission spot.

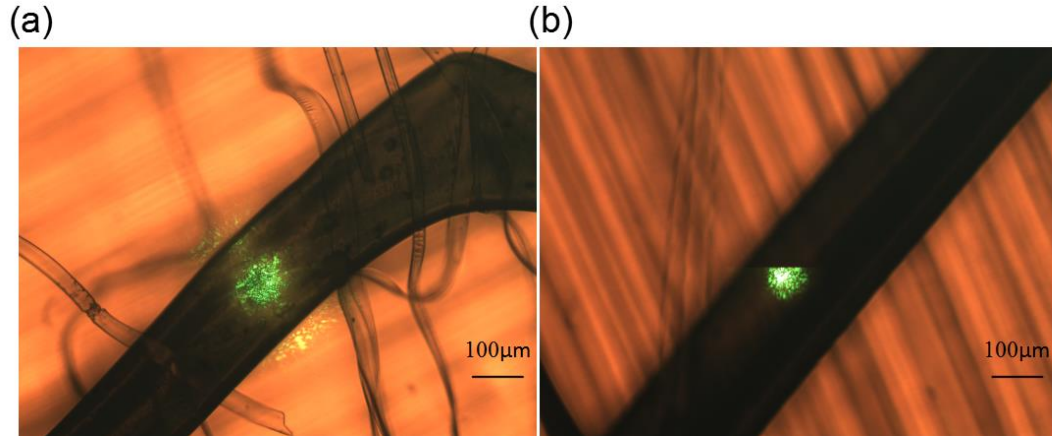


**Figure 1.** The optical images of two dye doped-electrospun fibers with the PM597/NB mass ratio of 0.67/1 (a) and 1.5/1 (b) under the pump of 532 nm pulse laser.

The emission spectra measurement setup was built based on the microscope system (Ideaoptics Co. Ltd) to obtain the detailed experimental data. As shown in Figure 2, a Q-switched Nd:YAG laser which outputs a Gaussian profile spot with a wavelength of 532 nm (pulse duration 10 ns, repetition rate 10 Hz, spot diameter 100  $\mu\text{m}$ ) is used to serve as pumping source. The pump pulse energy and polarization are controlled by a Glan Prism group. Two mirrors are employed to change the pumping laser path and guide the pumping laser into the microscope system. The pumping laser is totally reflected by a dichroic mirror and

focused onto the samples via an objective. Samples are excited by 532 nm laser to generate fluorescence emission/random lasing. The emitted light is collected by the same objective and passes through dichroic mirror with total transmission. Then the collected light is focused onto a beam splitter via the concave lens, where 50% of the light is sent to a CCD camera to obtain the images of the samples. The remaining 50% of the light is directly collected with a fiber-coupled spectrometer (QE65PRO, Ocean Optics, Inc., resolution  $\sim 0.4$  nm, integration time 100 ms).

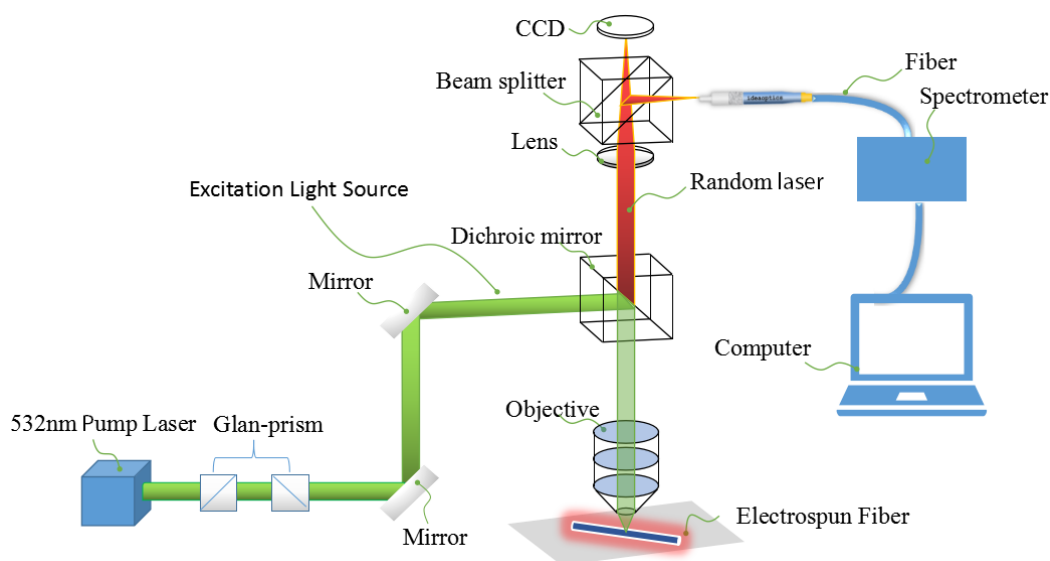


**Figure 2.** Microscope measurement setup. A Q-switched Nd:YAG laser which outputs a round-shape spot with a wavelength of 532 nm (pulse duration 10 ns, repetition rate 10 Hz, spot diameter 100  $\mu\text{m}$ ) is used to serve as pumping source. Fiber spectrometer (QE65PRO, ocean optics, resolution  $\sim 0.4$  nm, integration time 100 ms) is used to collect the emission spectra.

### 3. Results and discussions

To characterize the basic optical properties of the selected laser dyes, we firstly measured the absorption and fluorescence spectra of the donor dye (PM597), the acceptor dye (NB), and the mixed dye (PM597/NB), respectively. As shown in Figure 3(a), the mixture of PM597/NB exhibits two broad absorbance peaks with the wavelengths of 526.5 nm and 646 nm, which correspond to the absorbance peaks of the PM597 and NB dye, respectively. The basic requirement of constructing a FRET system is that the emission of the donor should have a good spectral overlap with the absorption of the acceptor.

Figure 3(b) shows the comparison between the emission spectrum of the PM597 and the absorption spectrum of the NB. It clearly shows that the two spectra have a good overlap in the wavelength range between 550 nm and 650 nm, indicating that the donor PM597 at excited state can effectively populate the acceptor NB at ground state via energy transfer process. It should be noticed that the absorption spectrum of the NB is a little far away from the 532 nm pump wavelength and does not fully cover the emission spectrum of the PM597. This is to prevent the acceptor (NB) from being directly excited by the pump laser.

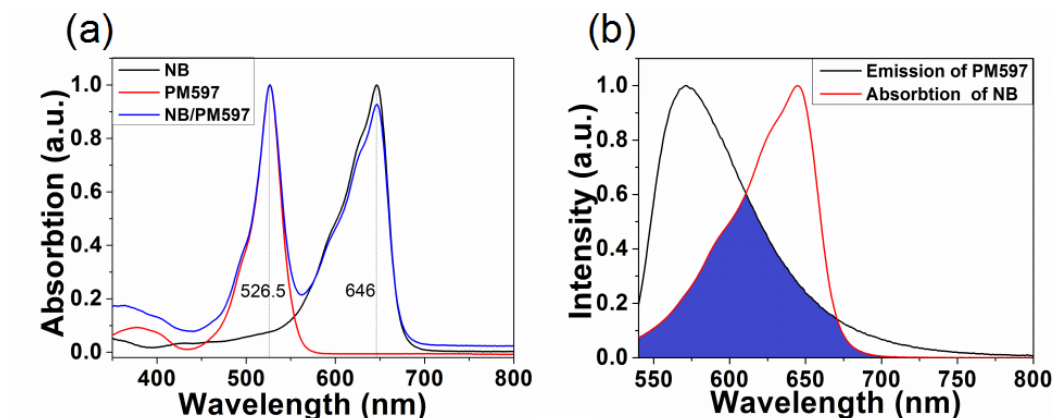


**Figure 3.** (a) The normalized absorption spectra of the donor dye PM597 (red), the acceptor dye NB (black), and the mixed dye of PM597/NB (blue), respectively. (b) The comparison between the normalized emission spectrum of the donor dye PM597 (black) and the normalized absorption spectrum of the acceptor dye NB (red), respectively. The blue shadow indicates the spectral overlap.

To verify whether the PM597 and NB dyes are suitable donor and acceptor for FRET process, the emission spectra of the PM597 dye, the NB dye, and the mixture of PM597/NB are measured, as shown in Figure 4(a). It can be seen that the PM597/NB mixture only contains one emission peak located at 674.4 nm matching the emission of the NB dye. This is because the PM597 dyes (donor) transfer their energy to the nearby NB dyes (acceptor) instead of directly emitting the fluorescence. As a consequence, the fluorescence from the excited NB dyes will dominate the emission spectrum of PM597/NB. This energy transfer process is the so-called FRET. The results imply that the mixture of PM597/NB dyes is an ideal gain

material for the construction of FRET system. In addition, we measure the fluorescence lifetime of PM597 mixed with and without NB as shown in Figure 4(b). The value of fluorescence lifetime  $L_f$  can be formulated as  $L_f = (T_{n=1,2} - T_0) / e$ , where  $T_0$ ,  $T_1$  and  $T_2$  are the time frames about 56.1 ns, 57.1 ns and 62.4 ns, respectively. As we can see, the presence of NB suppresses the lifetime of donor PM597, because the energy transfer between the donor and acceptor introduces additional non-radiative decay channel to the donor and result in a reduced lifetime. The lifetime results further confirmed that the FRET system has been successfully constructed based on the PM597 and NB dyes.

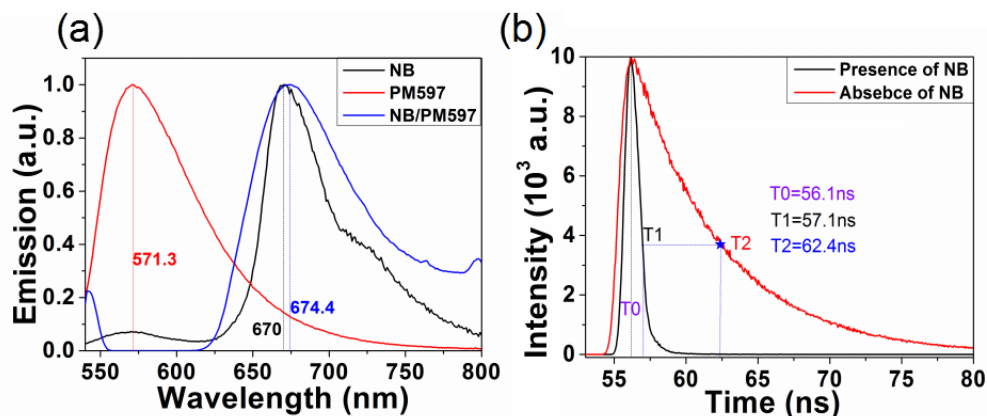


**Figure 4.** (a) The normalized emission spectra of the donor dye of PM597, the acceptor dye of NB, and the mixed dye of PM597/NB corresponding to the red, black and blue curve, respectively. (b) The luminescence decay curves of PM597 with (red curve) and without (black curve) NB.

A comprehensive study was carried out regarding to the fluorescence emission and random lasing performance of the electrospun polymer fibers with different PM597/NB dye ratio. The optimal FRET-assisted random lasing action was observed from the sample with the PM597/NB ratio of 0.67/1, as shown in Figure 5(a). The random lasing peaks centered at 683.5 nm dominant the whole lasing spectrum. As the ratio of PM597/NB increased, a new group of lasing peaks around 570 nm, corresponding to the emission of PM597, started to emerge in the emission spectrum, see in Figures 5(b) and 5(c). When the ratio of PM597/NB increased up to 3/1, the original random lasing peaks located in the emission band of NB degenerated to a weak fluorescence peak, whereas the random lasing peaks could be only found in the emission band of the PM597. This is because the FRET efficiency became weak as the proportion of the doped PM597 increased. The evaluation of the lasing spectra indicates that the variation of the donor-accepter ratio would influence the FRET efficiency and further switch the random

lasing wavelengths. The random lasing phenomenon observed in the electrospun polymer fiber results from the light multiple scattering caused by the inhomogeneity of the internal structure of the electrospun polymer fiber. Moreover, we also prepared a control sample with only NB. No random lasing can be observed in the control sample, because the absorption of NB is quite low at the standard pump wavelength (532 nm) and the NB dye cannot be excited without FRET process (see Figure S1 in the Supplemental Material Information). In view of this, the FRET-assisted electrospun polymer fiber RLs has been successfully demonstrated and its laser properties can be tuned via controlling the donor/accepter ratio.

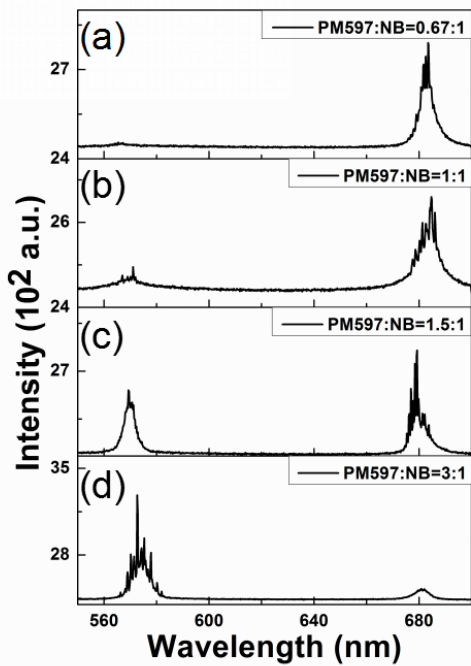


**Figure 5.** The energy transfer random lasing spectra from the samples with the PM597/NB ratio of 0.67/1 (a), 1/1 (b), 1.5/1 (c) and 3/1 (d).

To further study the optical properties of the FERT-assisted electrospun polymer fiber RLs, the emission spectra of the

above-mentioned four samples at different pump energy are measured, see results in Figures 6(a), 6(c), 6(e) and 6(g). For all the four samples, a broad spontaneous emission was observed at a low pump energy. When the pump energy increased over threshold, the multi-mode spike peaks began to emerge with the main peaks at wavelengths of 683.56 nm, 684.57 nm, 679.26 nm, and 572.68 nm, respectively. The dependence of the integrated peak emission intensities on the pump energy were extracted from the corresponding emission spectra, as shown in Figures 6(b), 6(d), 6(f) and 6(h). The integrating range are 672.83 nm-693.03 nm for the cases in Figures 6(b), 6(d) and 6(f) and 584.93 nm-563.84 nm for the case in Figure 6(h). Laser threshold behavior was observed in all four samples. Their laser threshold values were determined to be 132.5  $\mu\text{J}$ , 418.2  $\mu\text{J}$ , 315.5  $\mu\text{J}$ , and 40.93  $\mu\text{J}$ , respectively.

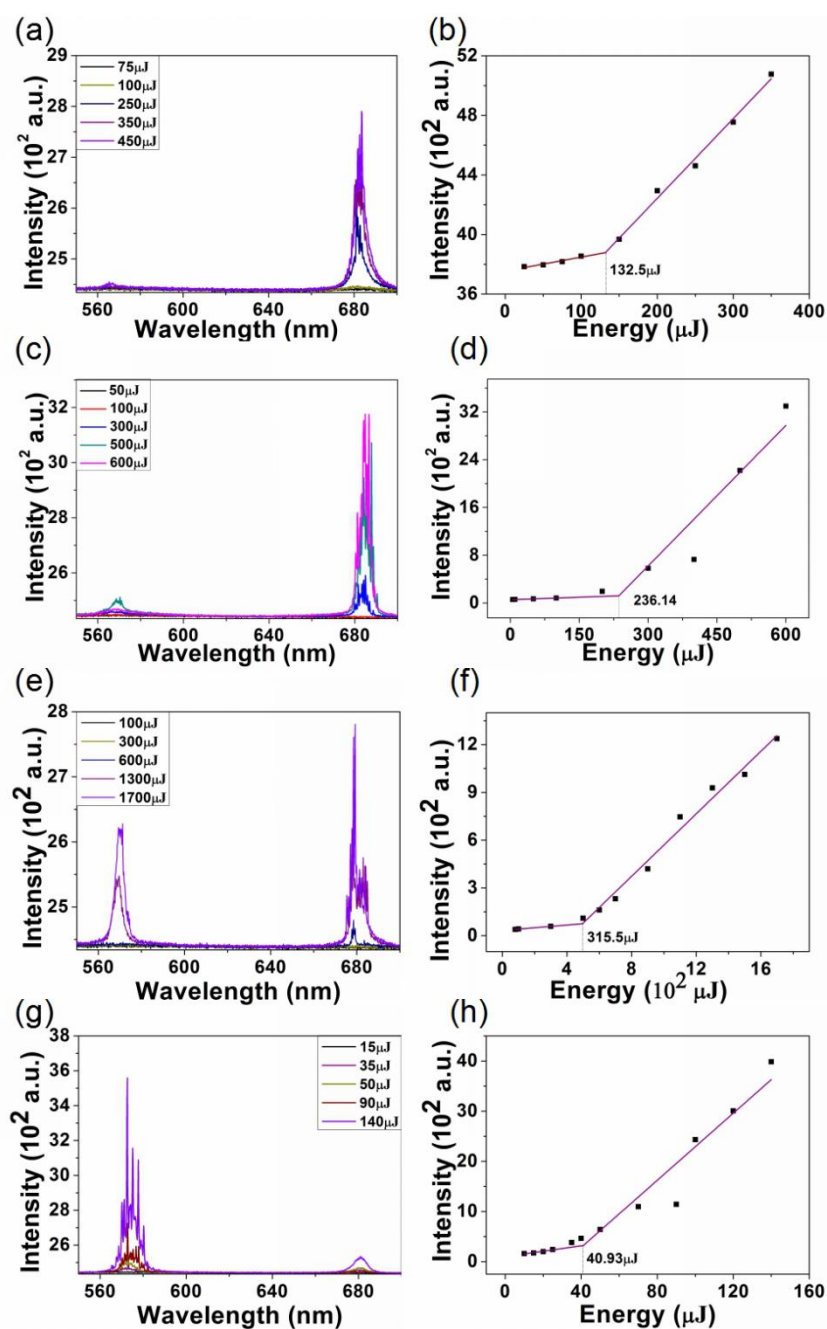


**Figure 6.** Spectral properties of the FRET-assisted RL. The emission spectra of the four samples with the PM597/NB ratio of 0.67/1 (a), 1/1 (c), 1.5/1 (e) and 3/1 (g) at different pump energy. The corresponding integrated emission intensities of the four samples with the PM597/NB ratio of 0.67/1 (b), 1/1 (d), 1.5/1 (f) and 3/1 (h) at different pump energy

In random system, this spectral fluctuation behavior is rich in the physical mechanism reflecting the influence of randomness and nonlinearity. Random lasing feedback is provided by the multiple light scattering, which may causes the randomness of the random laser emission direction. To this end, the lasing spectra of the sample with the

PM597/NB ratio of 0.67/1 were collected and the collection point is controlled to has a different distance from the pump region, see Figure 7. The corresponding collection configurations are shown in Figure S2 (see the Supplemental Material Information). The locations of the spectra detected points are determined by a probe light source. Figure

S3 (see the Supplemental Material Information) shows the post-section of the microscope, in which the emission spectra are collected by a fiber and analyzed by a spectrometer. After the spectra measurement, a halogen lamp is introduced in to the light path by a fiber coupler, working as a probe light. According to the reversibility principle of light path, the halogen lamp light spots (yellow spots in Figure S2) on the surface of the sample are the locations of the spectra detected points. Consequently, the separation distance between the pumping points and the spectra detected points can be determined. In Figure 7, we traced three main lasing peaks  $P_1$ - $P_3$  from the collected lasing spectra. It was found that the wavelengths of the lasing peaks are slight varied in different lasing spectra. For the lasing peak  $P_1$ , a  $\sim 0.3$  nm blue-shift (from 682.2 nm to 681.9 nm) has been observed in the spectrum collected with a distance of 229  $\mu\text{m}$  from the pump region. Meanwhile, the lasing peak  $P_2$  has a  $\sim 0.21$  nm red-shift (from 685.12 nm to 685.33 nm) in the case of 170  $\mu\text{m}$  separation distance. For the lasing peak  $P_3$ , it was absence in lasing spectra collected with a distance of 170  $\mu\text{m}$  and 193  $\mu\text{m}$  from the pump region. Such spectral variation can be attributed to the inhomogeneity of the electrospun and emitting directions of the excited random lasing modes.<sup>[43]</sup> As a result, through different collection points, the collected lasing modes are different.

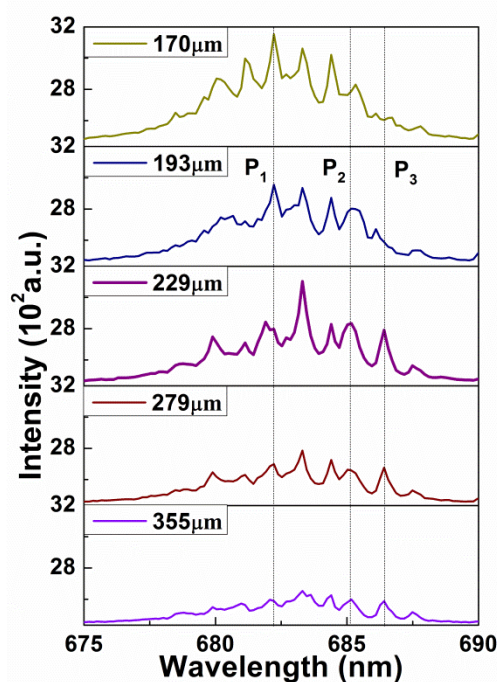


**Figure 7.** Characterization of the randomness in the FRET-assisted electrospun polymer fiber random lasing. The RL emission spectra for different reception location the electrospun polymer fiber with the PM597/NB ratio of 0.67/1.

The traditional RL systems with single gain materials has been demonstrated to exhibit an intrinsic feature of intensity fluctuation.<sup>[44]</sup> In our FRET-assisted electrospun polymer fiber RL, it contains two gain materials which form a multi-energy level system with the assistant of FRET process. To investigate whether such multi-energy level RL shows the similar feature, we measured the lasing properties for several times under the same experimental condition. Figure 8(a) shows the random lasing spectra from pulse to pulse pump for FRET-assisted electrospun polymer fiber RL with PM597/NB ratio of 0.67/1 at the same pump energy  $\sim 450$   $\mu\text{J}$ . It can be seen that the random lasing wavelengths remain unchanged, but their lasing intensities

vary from pulse to pulse. Moreover, we measured another sample with PM597/NB ratio of 1/1 and similar intensity fluctuation behavior was observed, as shown in Figure 8(b). These results indicated that our FRET-assisted electrospun polymer fiber RL is consisted

with the single gain RL system regarding to the intensity fluctuation. The physical mechanism of this intensity fluctuation behavior can be attribute to the strong competition and coupling between the numerous modes in the RL system.<sup>[45]</sup>

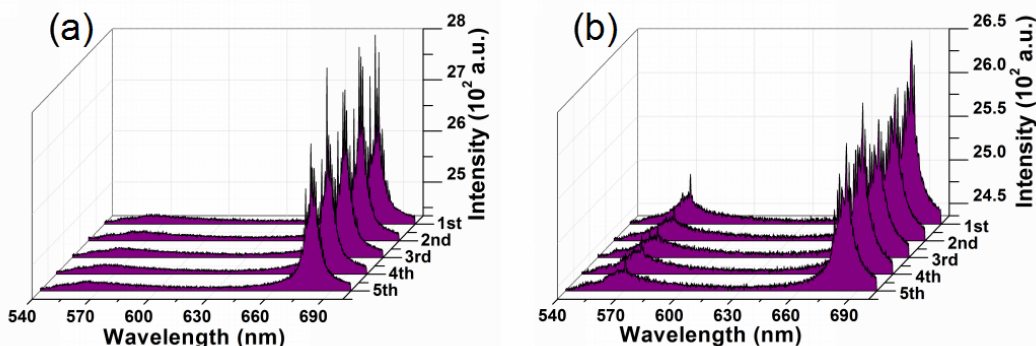


**Figure 8.** Demonstration of random lasing spectra fluctuation. The random lasing with different times pump with PM597/NB ratio of 0.67/1 (a) and 1/1(b).

Several recent studies have attempted to describe the dynamic of this intensity fluctuation phenomenon via the approach on the basis of spin glass theory.<sup>[35,46]</sup> The connection between spin-glass and RL is established on the account of the analogy between the continuous complex spin variables and the lasing modes. For a solid RL system, the scattering configuration is fixed and the disorder of the whole system does not change over time, termed quenched. According to the spin-glass theory, the intensity fluctuation (i.e. non-deterministic and irreproducible behavior of the laser modes) results from the frustration caused by the quenched disordered interaction, which corresponds to a glassy light behavior. During the transition to the glassy light regime, an important phenomenon, the so-called RSB has been observed in the single gain RL system, which reveals the non-trivial

modes organization and correlation.<sup>[34,37]</sup> To analyze the glassy behavior and possible RSB transition in the multi-gain RL system, we carried a statistical study based on our FRET-assisted electrospun polymer fiber RL using the replica method. The replica in spin-glass system stands for the identical system realizations under the same experimental condition. The RSB transition is characterized by the variation of the statistical distribution of Parisi overlap parameter which is associated with the system replica and reflects the interaction of the different states in a spin glass system. In the case of RL system, the theoretical replica is related with the amplitudes of the laser modes from the same RL system under the same pump energy in each shot. However, the phase information of the laser modes is not easy to be obtained in the experiments, which hinders the evaluation of the laser modes

amplitudes. The only experimentally accessible information of the laser modes is the intensity magnitudes. Thus, the real replica in RL system is defined as the lasing spectrum containing the laser modes intensities  $I_j \propto |a_j|^2$ , where  $a_j$  is the amplitude of the longitudinal mode  $j$ . Under each pump energy, we measure  $N_s$  system replicas (i.e. laser spectra). The intensity fluctuation overlap parameter  $q$ , an analogy to the Parisi parameter, is introduced and calculated as

$$q_{\alpha\beta} = \frac{\sum_{k=1}^N \Delta\alpha(k)\Delta\beta(k)}{\sqrt{\sum_{k=1}^N \Delta\alpha^2(k)}\sqrt{\sum_{k=1}^N \Delta\beta^2(k)}}$$

where  $\alpha, \beta=1, 2, \dots, N_s$  are the different replica indexes and  $\Delta_i(k)$  is the intensity fluctuation of the  $i$ -th replica at the wavelength index  $k$ .  $\Delta_i(k)$  is given by the equation  $\Delta_i(k) = I_i(k) - \bar{I}_i(k)$ .

The total number of the overlap parameter  $q$  is  $N_s(N_s-1)/2$ . Then, the distribution  $P(q)$  of the overlap parameters is analyzed to determine the The “ $q\alpha\beta$ ” is revised to “ $q_{\alpha\beta}$ ” system

regime. We first investigate the RSB transition in the FRET-assisted electrospun polymer fiber RLs with PM597/NB ratio of 0.67/1. For each pump energy, 1100 emission spectra are collected. The wavelength index  $k$  is in the range between 664.92 nm and 690.11 nm with a spectral resolution of 0.4 nm. Figure 9 shows the distributions  $P(q)$  of the overlap parameters calculated from emission spectra at different pump energy. It was found that the distribution  $P(q)$  are centered around  $q=0$  below the laser threshold, as shown in Figures 9(a)-9(b). This indicates that the modes are independent, corresponding to the RL system in an uncorrelated paramagnetic regime. As the pump energy increases, the distribution  $P(q)$  broadens and finally reaches the boundary of  $q=\pm 1$  with two humps (Figures 9(c)-9(d)). This suggests that the coupling between the laser modes becomes stronger and results in a non-trivial overlap distribution with the increasement of energy, which is referred as spin-glass phase. The variation from paramagnetic regime to spin-glass phase is a typical feature of the RSB transition.

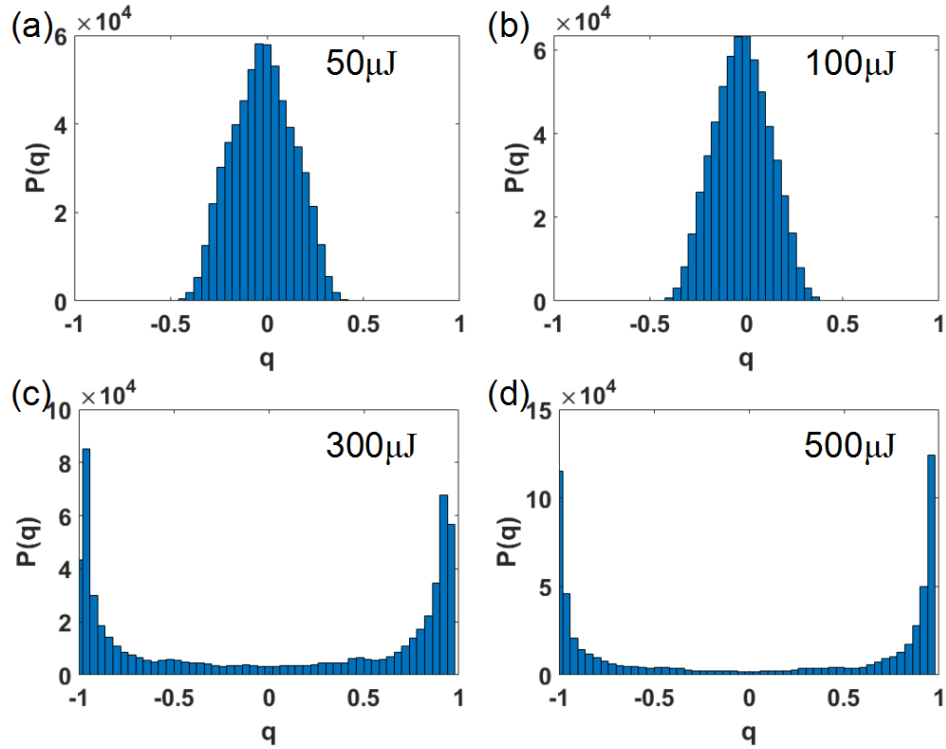


**Figure 9.** Distribution function of the overlap parameter  $q$  obtained from the FRET-assisted RL with PM597/NB ratio of 0.67/1 at the pump energy of 50  $\mu\text{J}$  (a), 100  $\mu\text{J}$  (b), 300  $\mu\text{J}$  (c), and 500  $\mu\text{J}$  (d).

To determine the relationship between RSB transition and the pump energy the dependency of the  $|q|_{\text{max}}$ , the  $q$  value of the maximum of  $P(|q|)$ , on the pump energy is calculated and plot in Figure 10(a). An abrupt increase of the  $|q|_{\text{max}}$  occurs at the pump energy of 130  $\mu\text{J}$ , denoting the RSB transition from a continuous wave paramagnetic regime to a spin-glass regime. It is interesting to find that this pump energy is just the laser threshold determined in Figure 6(b). Moreover, the glassy behavior in another two FRET-assisted electrospun polymer fiber RLs with the PM597/NB ratio of 1/1 and 1.5/1 was also studied. The corresponding results are shown in Figures S4 and S5 (see the Supplemental Material Information), respectively. The trend of the distribution  $P(q)$  obtained from these two samples is qualitatively the same with the first case, which proves

that RSB is always present in the FRET-assisted RLs. Based on analyzing the variation of the  $|q|_{\text{max}}$  at different pump energy, it was found that the RSB transition also occurs at the laser threshold, as shown in Figures 10(b)-10(c). This result is in consistent with the RSB transition in the single gain RL systems reported in previous studies. It seems that the existence of the two laser dyes and FRET process will not influence the glassy behavior and RSB transition in the RL system. This is because the duration time of the energy transfer is much smaller than the lifetime of the laser dyes and the total lifetime of the FRET system is similar as that of a single laser dye in the  $10^{-8}$  s timescale.<sup>[47]</sup> Compared with the total experiments time 20minutes (2 minutes for each set of measurement) in our case, the timescale of the FRET process is too small to

influence the randomness and the nonlinearity of the whole system.<sup>[41]</sup> Thus, the glassy behavior in the FRET-assisted RL shows no different with that in the single gain RL system. In addition, we conducted the glassy behavior in the sample with PM597/NB proportion of 3/1 (Figure S6 in the Supplemental Material Information). As mentioned in above section, this sample only generates the random lasing in the emission band of the PM597 and can be regarded as a traditional single-gain RL. The emission

spectra collected from the sample is selected in the spectral range between 550.8 nm and 575.14 nm. Similarly, the RSB transition from a continuous wave paramagnetic regime to a spin-glass phase is observed at the laser threshold (Figure 10(d)). In view of this, the RSB transition is robust in the RL system with and without FRET process, which can be regarded as an indicator of the laser threshold.

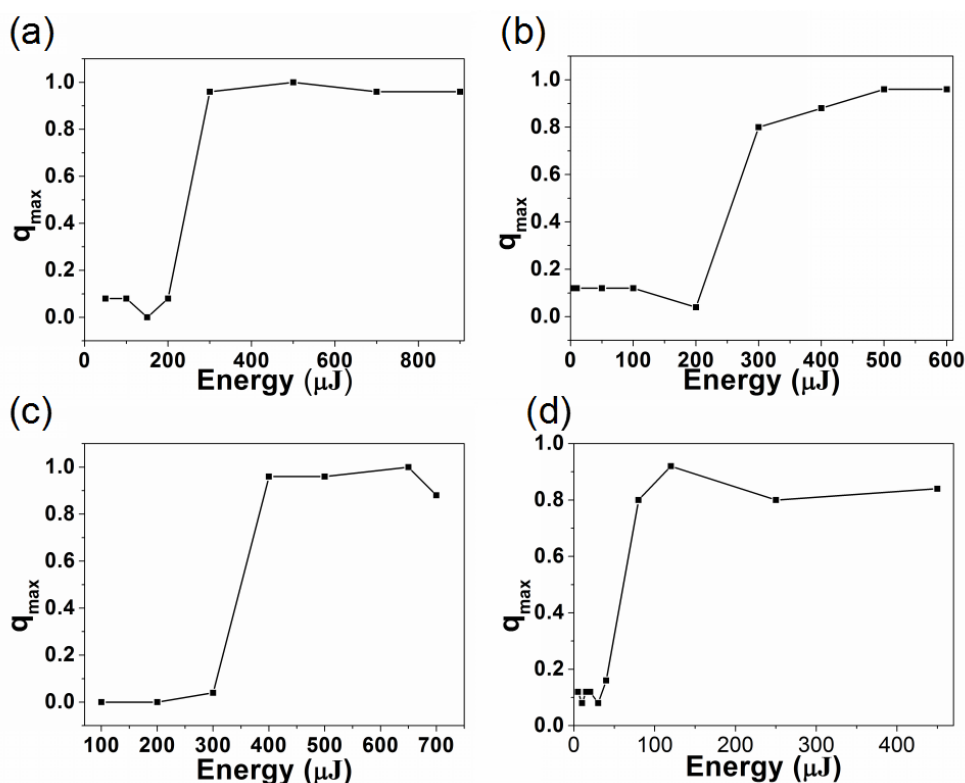


**Figure 10.** The parameter  $|q| = q_{\max}$  as a function of the pump energy for the samples with ratio of 0.67/1 (a), 1/1 (b), 1.5/1 (c) and 3/1 (d).

#### 4. Conclusion

To summary, we introduce an advanced technology – electrospun to construct a FRET-assisted RL system, which achieves efficient long-wavelength ( $\geq$

650 nm) random lasing at the standard pump wavelength (532 nm). The donor (pyromethene 597) and acceptor (nile blue) laser dyes are introduced to the as-fabricated electrospun micro-scale polymer fiber to form a FRET system.

Under the excitation of 532 nm pump laser, the energy transition from donor to acceptor is observed and it depends on the ratio between donor and acceptor. The optimal FRET random lasing is obtained from the electrospun polymer fiber RL with a PM597/NB ratio of 0.67/1. Our work provides a new approach to realize mass production of RLs with FRET process, promoting the development of RL for real application. Furthermore, based on the statistical study of the lasing properties in FRET-assisted electrospun polymer fiber RL, we observe the phase transition between a continuous wave paramagnetic regime (below threshold) and spin-glass regime (above threshold) representing RSB phenomenon. Our results prove that spin-glass theory can be used to describe the statistical properties of the FRET-assisted RL system, which open up new possibilities for the study of other glassy behaviors in the RL system with complex energy levels and energy cascaded process, for example, quantum cascade laser.

## Acknowledgments

The authors would like to thank the financial supports from National Natural Science Foundation of China (11874012, 11404087, 11574070, 51771186, 11404086, 11874126, 61501165); Fundamental Research Funds for the Central Universities (JZ2019HGPA0099; PA2018GDQT0006); Project of State Key Laboratory of Environment-friendly Energy Materials, Southwest University of Science and Technology (17FKSY0109); Anhui Province Key Laboratory of Environment-friendly Polymer Materials (KF2019001); the European Union's

Horizon 2020 research and innovation programme under the Marie Skłodowska-Curie grant agreement No 744817; STCSM; China Postdoctoral Science Foundation (2015M571917, 2017T100442).

## Conflict of Interest

The authors declare no conflict of interest.

## Keywords

Förster resonance energy transfer, electrospun polymer fiber, random laser, replica symmetry breaking

## References

- [1] N. M. Lawandy, R. M. Balachandran, *Nature*. **1995**, 373, 203.
- [2] D. S. Wiersma, M. P. Aan Albada, A. Lagendijk, *Nature*. **1995**, 373, 203.
- [3] D. S. Wiersma, *Nature* **2000**, 406, 132.
- [4] H. Cao, J. Xu, E. W. Seelig, R. P. H. Chang, *Appl. Phys. Lett.* **2000**, 76, 2997.
- [5] D. S. Wiersma, *Nat. Phys.* **2008**, 4, 359.
- [6] Y. Ling, H. Cao, A. L. Burin, M. A. Ratner, X. Lin, R. P. H. Chang, *Phys. Rev. A* **2001**, 64, 063808.
- [7] L. Ye, C. Lv, F. Li, Y. Wang, B. Liu, Y. Cui, *J. Mod. Optic.* **2017**, 64, 1429.
- [8] Q. Song, S. Xiao, X. Zhou, L. Liu, L. Xu, Y. Wu, Z. Wu, *Opt. Lett.* **2007**, 32, 373.
- [9] D. Cao, D. Huang, X. Zhang, S. Zeng, J. Parbey S. Liu, C. Wang, T. Yi, T. Li, *Laser Phys.* **2018**, 28, 025801.
- [10] L. Cerdán, A. Costela, G. Durán-Sampedro, I. García-Moreno, *Appl. Phys. B* **2012**, 108, 839.
- [11] L. Yin, Y. Liang, B. Yu, Y. Wu, J. Ma, K. Xie, W. Zhang, G. Zou, Z. Hu, Q.

- Zhang, *RSC Adv.* **2016**, *6*, 98066.
- [12] L. Yin, Y. Liang, B. Yu, Y. Wu, J. Ma, K. Xie, W. Zhang, G. Zou, Z. Hu, Q. Zhang, *RSC Adv.* **2016**, *6*, 85538.
- [13] Z. Hu, J. Xia, Y. Liang, J. Wen, E. Miao, J. Chen, S. Wu, X. Qian, H. Jiang, K. Xie, *Opt. Express* **2017**, *25*, 18421.
- [14] Z. Hu, Y. Liang, P. Gao, H. Jiang, J. Chen, S. Jiang, K. Xie, *J. Opt.* **2015**, *17*, 125403.
- [15] S. Kedia, S. Sinha, *Results in Physics*, **2017**, *7*, 697-704.
- [16] H. Lu, J. Xing, C. Wei, J. Xia, J. Sha, Y. Ding, G. Zhang, K. Xie, L. Qiu, Z. Hu, *Photonics Research*, **2018**, *6*, 390-395.
- [17] A. Mooradian, T. Jaeger, P. Stokseth, *Springer*, **1976**.
- [18] H. P. Berlien, G. J. Müller, *J. Biomed. J. Biomed. Opt.* **2004**, *9*, 844.
- [19] B. Azzedine, C. Mahmoud, F. Alexis, *An Introduction to Organic Lasers* Elsevier, Netherlands **2017**.
- [20] T. Förster, *Ann. Phys-Berlin* **1948**, *437*, 55.
- [21] J. F. Galisteolópez, M. Ibisate, C. López, *J. Phys. Chem. C* **2014**, *118*, 9665.
- [22] L. Cerdán, E. Enciso, V. Martín, J. Bañuelos, I. López-Arbeloa, A. Costela, I. Garacía-Moereno, *Nat. Photonics* **2013**, *6*, 623.
- [23] X. Shi, J. Tong, D. Liu, Z. Wang, *Appl. Phys. Lett.* **2017**, *110*, 171110.
- [24] V. Vohra, A. Devaux, L. Q. Dieu, G. Scavia, M. Catellani, G. Calzaferri, C. Botta, *Adv. Mater.* **2010**, *21*, 1146.
- [25] C. Kuo, C. Wang, W. Chen, *Macromol. Mater. Eng.* **2008**, *293*, 999.
- [26] X. Wang, C. Drew, S. Lee, K. J. Senecal, J. Kumar, L. A. Samuelson, *Nano Lett.* **2002**, *2*, 1273.
- [27] Y. Jun, E. Kang, S. Chae, S. Lee, *Lab. Chip.* **2014**, *14*, 2145.
- [28] S. Agarwal, J. Wendorff, A. Greiner, *Adv. Mater.* **2009**, *21*, 3343.
- [29] L. Sznitko, L. Romano, A. Camposeo, D. Wawrzynczyk, K. Cyprych, J. Mysliwiec, D. Pisignano, *J. Phys. Chem. C* **2017**, *122*, 09125.
- [30] V. Vohra, G. Calzaferri, S. Destri, M. Pasini, W. Porzio, C. Botta, *Acs Nano* **2010**, *4*, 1409.
- [31] J. L. van Hemmen, *Phys. Rev. A Gen. Phys* **1986**, *34*, 3435.
- [32] L. M. Duan, E. Demler, M. D. Lukin, *Phys. Rev. Lett.* **2003**, *91*, 090402.
- [33] D. S. Wiersma, *Nat. Photonics* **2013**, *7*, 188.
- [34] A. S. L. Gomes, B. Lima, P. R. Pincheira, A. L. Moura, M. Gagné, E. P. Raposo, C. D. Araujo, R. Kashyap, *Phys. rev. A* **2016**, *94*, 011801.
- [35] L. Angelani, C. Conti, G. Ruocco, F. Zamponi, *Rev. Lett.* **2006**, *96*, 065702.
- [36] L. Angelani, C. Conti, G. Ruocco, F. Zamponi, *Phys. Rev. B* **2006**, *74*, 104207.
- [37] N. Ghofraniha, I. Viola, F. D. Maria, G. Barbarella, G. Gigli, L. Leuzzi, C. Conti, *Nat. Commun.* **2015**, *6*, 7058.
- [38] F. Antenucci, A. Crisanti, L. Leuzzi, *Phys. Rev. A* **2015**, *91*, 8706.
- [39] B. C. Lima, A. S. L. Gomes, P. I. R. Pincheira, A. L. Moura, M. Gagné, E. P. Raposo, C. B. de Araújo, R. Kashyap, *J. Opt. Soc. Am. B* **2017**, *34*, 293-299.
- [40] F. Tommasi, E. Ignesti, S. Lepri, S. Cavalieri, *Sci. Rep.* **2016**, *6*, 37113.
- [41] P. I. R. Pincheira, S. F. Andréa, S. I. Fewo, S. J. M. Carreno, A. L. Moura, E. P. Raposo, A. S. L. Gomes, C. de Araujo, *Opt. Lett.* **2016**, *41*, 3459.
- [42] S. Krämmmer, C. Vannahme, C. L. C. Smith, T. Grossmann, M. Jenne, S. Schierle, L. Jørgensen, L. S. Chronakis, A. Kristensen, H. Kalt, *Adv. Mater.* **2014**, *26*, 8096.
- [43] T. Hisch, M. Liertzer, D. Pogany, F. Mintert, S. Rotter, *Phys. Rev. Lett.* **2013**, *111*, 023902.

- [44] Z. Hu, B. Miao, T. Wang, Q. Fu, D. Zhang, H. Jiang, Q. Zhang, *Opt. Lett.* **2013**, *38*, 4644.
- [45] J. W. Merrill, H. Cao, E. R. Dufresne, *Phy. Rev. A* **2015**, *93*, 021801.
- [46] F. Antenucci, C. Conti, A. Crisanti, L. Leuzzi, *Phys. Rev. Lett.* **2015**, *114*, 043901.
- [47] J. R. Lakowicz, *Principles of Fluorescence Spectroscopy* Plenum Press, New York **2006**.